Reduced nicotinamide mononucleotide is a new and potent nad+ precursor in mammalian cells and mice

Zapata-Pérez, Rubén; Tammaro, Alessandra; Schomakers, Bauke V.; Scantlebery, Angelique M. L.; Denis, Simone; Elfrink, Hyung L.; Giroud-Gerbetant, Judith; Cantó, Carles; López-Leonardo, Carmen; McIntyre, Rebecca L.; van Weeghel, Michel; Sánchez-Ferrer, Álvaro; Houtkooper, Riekelt H.

Published in:
FASEB journal

DOI:
10.1096/fj.202001826R

Published: 01/04/2021

Document Version
Publisher's PDF, also known as Version of record

Citation for pulished version (APA):
Zapata-Pérez, R., Tammaro, A., Schomakers, B. V., Scantlebery, A. M. L., Denis, S., Elfrink, H. L., Giroud-Gerbetant, J., Cantó, C., López-Leonardo, C., McIntyre, R. L., van Weeghel, M., Sánchez-Ferrer, Á., & Houtkooper, R. H. (2021). Reduced nicotinamide mononucleotide is a new and potent nad+ precursor in mammalian cells and mice. *FASEB journal*, *35*(4), 1-17. Article e21456. https://doi.org/10.1096/fj.202001826R

Received: 27 July 2020 | Revised: 1 February 2021 | Accepted: 2 February 2021

DOI: 10.1096/fj.202001826R

RESEARCH ARTICLE

THE FASEB JOURNAL

Reduced nicotinamide mononucleotide is a new and potent NAD^+ precursor in mammalian cells and mice

Rubén Zapata-Pérez[1] | Alessandra Tammaro[2] | Bauke V. Schomakers[1,3] | Angelique M. L. Scantlebery[1] | Simone Denis[1] | Hyung L. Elfrink[1,3] | Judith Giroud-Gerbetant[4] | Carles Cantó[4] | Carmen López-Leonardo[5] | Rebecca L. McIntyre[1] | Michel van Weeghel[1,3] | Álvaro Sánchez-Ferrer[6] | Riekelt H. Houtkooper[1]

[1]Laboratory Genetic Metabolic Diseases, Amsterdam Gastroenterology, Endocrinology, and Metabolism, Amsterdam Cardiovascular Sciences, Amsterdam UMC, University of Amsterdam, Amsterdam, The Netherlands

[2]Pathology Department, Amsterdam UMC, University of Amsterdam, Amsterdam, The Netherlands

[3]Core Facility Metabolomics, Amsterdam UMC, University of Amsterdam, Amsterdam, the Netherlands

[4]Nestlé Institute of Health Sciences, Nestlé Research, Lausanne, Switzerland

[5]Department of Organic Chemistry, University of Murcia, Murcia, Spain

[6]Department of Biochemistry and Molecular Biology-A, University of Murcia, Murcia, Spain

Correspondence
Rubén Zapata-Pérez and Riekelt H. Houtkooper, Laboratory Genetic Metabolic Diseases, Amsterdam Gastroenterology, Endocrinology, and Metabolism, Amsterdam Cardiovascular Sciences, Amsterdam UMC, University of Amsterdam, Meibergdreef 9, Amsterdam, The Netherlands.

Abstract

Nicotinamide adenine dinucleotide (NAD^+) homeostasis is constantly compromised due to degradation by NAD^+-dependent enzymes. NAD^+ replenishment by supplementation with the NAD^+ precursors nicotinamide mononucleotide (NMN) and nicotinamide riboside (NR) can alleviate this imbalance. However, NMN and NR are limited by their mild effect on the cellular NAD^+ pool and the need of high doses. Here, we report a synthesis method of a reduced form of NMN (NMNH), and identify this molecule as a new NAD^+ precursor for the first time. We show that NMNH increases NAD^+ levels to a much higher extent and faster than NMN or NR, and that it is metabolized through a different, NRK and NAMPT-independent, pathway. We also demonstrate that NMNH reduces damage and accelerates repair in renal tubular epithelial cells upon hypoxia/reoxygenation injury. Finally, we find that NMNH administration in mice causes a rapid and sustained NAD^+ surge in whole blood, which is accompanied by increased NAD^+ levels in liver, kidney, muscle, brain, brown adipose tissue, and heart, but not in white adipose tissue. Together, our data highlight NMNH as a new NAD^+ precursor with therapeutic potential for acute kidney injury, confirm the existence of a novel pathway for the recycling of reduced NAD^+ precursors and establish NMNH as a member of the new family of reduced NAD^+ precursors.

KEYWORDS

metabolism, NAD^+, NMNH, nicotinamide mononucleotide

Abbreviations: AK, adenosine kinase; AKI, acute kidney injury; ENT, equilibrative nucleoside transporter; ETC, electron transport chain; IR, ischemia reperfusion; NA, nicotinic acid; NAD^+, nicotinamide adenine dinucleotide; NADH, reduced nicotinamide adenine dinucleotide; NADS, NAD^+ synthase; NAM, nicotinamide; NAMPT, nicotinamide phosphoribosyltransferase; NAPRT, nicotinic acid phosphoribosyltransferase; NMN, nicotinamide mononucleotide; NMNAT, nicotinamide mononucleotide adenylyl transferase; NMNH, reduced nicotinamide mononucleotide; NR, nicotinamide riboside; NRH, reduced nicotinamide riboside; NRK, nicotinamide riboside kinase; PARP, poly (ADP-ribose) polymerase; PPP, pentose phosphate pathway; PRPP, phosphoribosyl pyrophosphate; TECs, tubular epithelial cells.

Funding information
NWO-FAPESP, Grant/Award Number: 457002002; European Union's Horizon 2020; Marie Skłodowska-Curie, Grant/Award Number: 840110; ERC Starting grant, Grant/Award Number: 638290; ZonMw, Grant/Award Number: 91715305; Velux Stiftung, Grant/Award Number: 1063; MINECO-FEDER, Grant/Award Number: BIO2013-45336-R; Ayudas a los Grupos y Unidades de Excelencia Científica de la Región de Murcia, Fundación Séneca- Agencia de Ciencia y Tecnología de la Región de Murcia, Grant/Award Number: 19893/GERM/15

1 | INTRODUCTION

Nicotinamide adenine dinucleotide (NAD^+) and its reduced form (NADH) are ubiquitous molecules in the body, which play crucial roles in energy metabolism, as they act as hydride-accepting and hydride-donating coenzymes during mitochondrial oxidative phosphorylation.[1] Apart from its role as a redox cofactor, during the last decade NAD^+ has arisen as the critical substrate for a number of protein families, such as the sirtuin (SIRT) family of protein deacetylases,[2] poly(ADP-ribose)polymerases,[3] and ADP-ribose cyclases.[4] Through their downstream actions, these proteins participate in more than 500 enzymatic reactions and regulate almost all major biological processes in cells.[5] This continuous enzymatic utilization of NAD^+ is counterbalanced via de novo synthesis from dietary tryptophan, or through its salvage from precursors. In the Preiss-Handler pathway, the NAD^+ precursor nicotinic acid (NA) is converted into NAD^+ in a three-step enzymatic process led by the nicotinic acid phosphoribosyltransferase (NAPRT), the nicotinamide mononucleotide adenylyl transferases (NMNATs), and the NAD^+ synthase (NADS). Another recycling pathway comprises intracellular nicotinamide (NAM) phosphoribosylation or nicotinamide riboside (NR) phosphorylation into nicotinamide mononucleotide (NMN), a process carried out by nicotinamide phosphoribosyltransferase (NAMPT) or nicotinamide riboside kinases (NRKs), respectively. NMN is then directly converted to NAD^+ by the NMNATs.[6] When given externally, NMN can also act as an NAD^+ precursor. To achieve this, NMN first needs to be converted extracellularly to NR by the ectoenzyme 5′-nucleotidase CD73, after which NR is transported into the cell by the equilibrative nucleoside transporters (ENTs) and metabolized to NAD^+ via NRKs.[7,8] Very recently, it has also been reported that NMN can be incorporated into cells via the Slc12a8-specific transporter, at least in mouse small intestine.[9]

The role of NAD^+ in the activity of enzymes controlling major metabolic processes, together with reports supporting that decreased cellular NAD^+ contributes to metabolic disturbances,[10] have renewed the interest in strategies to increase NAD^+ bioavailability to combat disease. In fact, NAD^+ repletion and the subsequent activation of sirtuins leads to key biochemical and clinical improvements, such as enhanced mitochondrial biogenesis,[11-14] protection against fatty acid-induced liver disease[15] and diabetes,[11,12] or reduced neurodegeneration[16] in a variety of animal models. NAD^+ homeostasis also plays a major role in kidney health and in the ability of the renal tubule to resist stressors.[17] In fact, during ischemic renal injury, NAD^+ consumption by poly (ADP-ribose) polymerases (PARPs) is accelerated,[18] leading to NAD^+ decline in renal tissue. NAD^+ replenishment through administration of the NAD^+ precursor NMN has been proven effective in ameliorating tubular damage induced by ischemia-reperfusion (IR) injury and the nephrotoxic drug cisplatin in aged mice.[19]

These results have turned attention to the use of NAD^+ precursors for combatting metabolic disease in humans. NA and NAM have downsides, however. The former induces flushing triggered by NA binding to the GPR109A receptor,[20] and NAM can act as a sirtuin inhibitor, which could limit its intended activation of these enzymes. Therefore, NMN and NR have arisen as attractive alternatives to NA or NAM, since they effectively raise NAD^+ concentrations in mouse tissues without undesired adverse target effects.[11,12,21,22] For this reason, several clinical studies have been initiated with NR. Some studies[23-28] with NR have shown that this compound is well tolerated up to 2 g per day during 12 weeks, while the first clinical trials with NMN are still ongoing (NCT03151239, UMIN000021309, UMIN000030609, and UMIN000025739). Yet, NMN and NR supplementation have some limitations of their own, including maximal NAD^+-enhancing effects of around 2-fold, the need of high doses (from 200 to 1000 mg/kg per day) to achieve beneficial effects in animal models,[11-13,22,29] and the rapid degradation in plasma to NAM, at least in the case of NR.[30] Moreover, although an increase in NAD^+ levels in whole blood has been detected upon NR administration in humans,[24,27] supplementation with this precursor has failed to increase NAD^+ in other tissues, such as muscle biopsies, even after 1 g administration

during 6 weeks.[31] This inefficacy in raising NAD^+ might explain why NR has no apparent effect on total energy expenditure, blood glucose or insulin sensitivity in humans.[28]

To overcome the limitations of the current repertoire of NAD^+ enhancers, other molecules with a more pronounced effect on the NAD^+ intracellular pool are desired. This has stimulated us to investigate the use of the reduced form of nicotinamide mononucleotide (NMNH) as an NAD^+ enhancer. There is very scarce information about the role of this molecule in cells. In fact, only one enzymatic activity has been described to produce NMNH. This is the NADH diphosphatase activity of the human peroxisomal Nudix hydrolase hNUDT12[32] and the murine mitochondrial Nudt13.[33] It has been postulated that, in cells, NMNH would be converted to NADH via nicotinamide mononucleotide adenylyl transferases (NMNATs).[34] However, both NMNH production by Nudix diphosphatases and its use by NMNATs for NADH synthesis have only been described in vitro using isolated proteins, and how NMNH participates in cellular NAD^+ metabolism remains unknown.

In the present study, we design and develop a new method for the purification of NMNH at scale, and explore the role of this molecule in NAD^+ metabolism. We show that NMNH is effectively metabolized to NAD^+ in mammalian cells, and confirm its NAD^+ synthesis route is NRK and NAMPT-independent. We also investigate the therapeutic potential of NMNH, showing that it can protect renal proximal tubular epithelial cells from hypoxia/reoxygenation-induced injury, a crucial event in ischemic acute kidney injury (AKI),[35] by accelerating processes involved in tubular regeneration.[36] Finally, we explore the in vivo effects of NMNH administration in mice and demonstrate that this new precursor effectively raises NAD^+ levels in blood and a variety of tissues, including kidney, to a greater extent than NMN when used at the same concentration.

These results corroborate that reduced NAD^+ precursors can act as very potent NAD^+ enhancers, and open doors for a new generation of highly efficient NAD^+-boosting molecules that could aid in overcoming the limitations of the current set of NAD^+ enhancers.

2 | MATERIALS AND METHODS

2.1 | Enzyme preparation and NMNH synthesis

The pyrophosphatase from *Escherichia coli* strain K12 (EcNADD, Uniprot code: P32664) was cloned into pET24b vector and expressed in *E coli* Rosetta 2 DE3 pLysS at 25°C and 0.25 mM of isopropyl-β-thiogalactopyranoside (IPTG, Sigma-Aldrich, St. Louis, MO, USA) for 16 hours. Protein purification was performed in a HiTrap IMAC column (GE Healthcare) in 50 mM of Tris-HCl pH 7.5 containing 300 mM of NaCl in a gradient from 10 to 250 mM of imidazole followed by desalting in a HiPrep desalting column (GE Healthcare, Chicago, IL, USA). Conversion of NADH into NMNH and AMP was achieved by incubation of 50 μg/mL EcNADD with 5 mM NADH in 50 mM Tris HCl pH 8.0 containing 0.5 mM $MnCl_2$ in a total volume of 50 mL for 45 minutes at 37°C. NADH conversion was checked by HPLC using a reverse-phase C_{18} 250 × 4.6 mm column (Phenomenex, Torrance, CA, USA) and a mobile phase consisting of 20 mM ammonium acetate pH 6.9 running at 1 mL/min for 15 minutes. Under these chromatographic conditions, retention times for NMNH and AMP were 5.5 and 7 minutes, respectively.

2.2 | NMNH purification

Chromatographic separation of NMNH from AMP was achieved by C_{18} reverse-phase chromatography. Fractions containing pure NMNH were evaporated until dryness in a rotary evaporator. The resulting powder was redissolved and desalted by size exclusion chromatography in pure water. After the final desalting step, samples were freeze dried to obtain NMNH as an amorphous yellow powder.

2.3 | Identification of NMNH by nuclear magnetic resonance

The proton and ^{31}P NMR spectra were recorded at 25°C on a Bruker (Billerica, MA, USA) Avance 400 (400 MHz). ^1H chemical shifts were reported in ppm relative to the resonance of HOD ($\delta = 4.8$ ppm) and ^{31}P chemical shifts were externally referenced to 85% of H_3PO_4. *J* values are given in Hz.

2.4 | Cell culture and supplementation with NAD^+ precursors

AML12, HepG2, SY5Y, HeLa cells, and human skin fibroblasts were cultured in 12-well plates in Dulbecco's modified Eagle's medium (DMEM, Life Technologies, Carlsbad, CA, USA) supplemented with 10% of fetal bovine serum (FBS, BioWhittaker, Basel, CH), 100 U/mL of penicillin, and 10 mg/mL of streptomycin (Life Sciences, Waltham, MA, USA). T37i cells were cultured and differentiated as previously described.[37,38] Conditionally Immortalized Proximal Tubular Epithelial Cells (IM-PTECs) were generated as previously described[39] and cultured at 33°C in HK2 medium[40] supplemented with 10 ng/mL IFN-γ (ProSpec, Rehovot, IL, USA) and maintained at 37°C without IFN-γ for an additional week before the start of the assay, resulting in loss

of SV40 expression.[41] Otherwise indicated, supplementation with PBS (vehicle), NMN (Carbosynth, Compton, UK), or NMNH was made at the concentrations and times indicated in FBS-free medium.

Chemical inhibition of the different enzymes involved in the recycling of NAD^+ precursors was made using the following reagents and concentrations: (E)-N-[4-(1-benzoylpiperidin-4-yl)butyl]-3-(pyridin-3-yl) acrylamide (FK866; 2 μM; Sigma-Aldrich), adenosine-5′-[(α,β)-methylene]diphosphate (AOPCP; 500 μM; Jena Biosciences, Jena, DE), dipyridamole (DIPY; 20 μM; Sigma-Aldrich), 5-(3-Bromophenyl)-7-[6-(4-morpholin yl)-3-pyrido[2,3-d]pyrimidin-4-amine dihydrochloride (ABT702; 10 μM; Tocris Biosciences, Bristol, UK), and gallotannin (100 μM; Sigma-Aldrich). Cells were incubated for 1 hour in the presence of the corresponding inhibitor prior to supplementation with the indicated concentrations of NMNH or PBS (vehicle).

2.5 | Viability assay

AML12 cells were cultured in DMEM in a 96-well plate and supplemented with different concentrations of NMN or NMNH. After 24 hours, cells were washed with PBS and 150 μL of MTS reagent (Abcam, Cambridge, UK) was added to each well. After incubation at 37°C for 4 hours, absorbance was measured on a spectrophotometer at 490 nm.

2.6 | Enzymatic cyclic assay for quantitative NAD^+ determination

For NAD^+ extraction, cells were washed twice with PBS, quenched with 400 μL of 2 M $HClO_4$ and transferred to 1.5 mL tubes. For tissues, 3-4 mg of freeze-dried tissue or 10 μL of blood were resuspended in 400 μL of 2 M $HClO_4$ and disrupted using a TissueLyser (Qiagen, Venlo, NL) for 5 minutes at 30 pulses per second. After centrifugation at 16 000 *g* for 5 minutes, 100 μL of the acidic supernatant was neutralized by addition of 150 μL 2 M/0.6 M KOH/MOPS and centrifuged again to remove precipitated salts. NAD^+ content was determined using an enzymatic spectrophotometric cycling assay based on the coupled reaction of malate and alcohol dehydrogenases, as previously described.[42]

2.7 | Mass spectrometry measurements

PBS-washed cells or 5-6 mg of freeze-dried tissue were metabolically quenched using ice-cold methanol (500 μL) and diluted with Milli-Q water (500 μL) containing internal standards, D_5-glutamine, D_5-phenylalanine, adenosine-$^{15}N_5$-monophosphate, adenosine-$^{15}N_5$-triphosphate, and guanine-$^{15}N_5$-triphosphate (5 μM each). Phase separation was performed by chloroform addition (1 mL) followed by thorough mixing. The homogenate was centrifuged at 16 000 *g* for 5 minutes at 4°C and the polar upper phase was transferred to a new 1.5 mL tube. Samples were then dried in a vacuum concentrator and pellets dissolved in 100 μL of methanol/water (6/4; v/v).

Metabolite analysis was carried out in an Acquity UPLC system (Waters, Milford, MA, USA) coupled to an Impact II Ultra-High Resolution Qq-Time-Of-Flight mass spectrometer (Bruker). Chromatographic separation of the compounds was achieved using a SeQuant ZIC-cHILIC column (PEEK 100 × 2.1 mm, 3 μm particle size; Merck, Kenilworth, NJ, USA) at 30°C. The LC method consisted in a gradient running at 0.25 mL/min from 100% mobile phase B (9:1 acetonitrile:water with 5 mM ammonium acetate pH 8.2) to 100% mobile phase A (1:9 acetonitrile:water with 5 mM ammonium acetate pH 6.8) in 28 minutes, followed by a re-equilibration step at 100% B of 5 minutes. MS data were acquired both in negative and positive ionization modes over the range of m/z 50-1200. Data from full-scan MS mode was analyzed using Bruker TASQ software (Version 2.1.22.1 1065). All reported metabolite intensities were normalized to total protein content in samples, determined using a Pierce BCA Protein Assay Kit, as well as to internal standards with comparable retention times and response in the MS. For MS/MS mode, the parent mass in positive mode was selected at m/z 335.1 ± 0.5 for NMN and m/z 337.1 ± 0.5 for NMNH both at 10 eV collision energy using ultrapure nitrogen as collision gas. Parent and subsequent daughter fragments were analyzed using Bruker Compass DataAnalysis (Version 5.1, Build 201.2.4019).

2.8 | Hypoxia/reoxygenation assays

In order to establish an in vitro model of tubular injury induced by hypoxia/reoxygenation, IM-PTECs were grown under oxygen-deficient conditions (1% O_2 and 5% CO_2 at 37°C) for 48 hours using a hypoxic incubator (HypOxystation H35; Don Whitley Scientific, Bingley, UK). Normoxic control cells were cultured under standard conditions (21% O_2 and 5% CO_2 at 37°C). After 48 hours, both hypoxic and normoxic cells received fresh HK2 medium, were cultured for an additional 24 hours under standard conditions (reoxygenation) and supplemented with the corresponding compounds, as indicated in the figure legends.

2.9 | Mitochondrial superoxide measurements

To examine the effect of NAD^+ boosting during hypoxia/reoxygenation on mitochondrial superoxide production, IM-PTECs were labeled with 5 μM of MitoSox Red (Thermo Fisher Scientific, Waltham, MA, USA) in HBSS supplemented with calcium and magnesium (Gibco, Waltham, MA, USA) for 10 minutes at 37°C. Relative fluorescence was measured by FACS.

2.10 | BrdU incorporation assay

To analyze the cell cycle, TECs subjected to hypoxia/reoxygenation conditions were incubated for 1 hour with 20 mM of bromodeoxyuridine (BrdU), and subsequently fixed in ice-cold ethanol. Cells were then incubated with 0.4 mg/mL of pepsin and 0.2 mM of HCl for 30 minutes at 37°C, followed by incubation with 2 M HCl for 25 minutes at 37°C. After washing, cells were stained for 30 minutes with anti BrdU-FITC (clone B44, BD Biosciences, San Jose, CA, USA) in PBS supplemented with 0.05% of Tween-20 and 0.5% of BSA. Finally, cells were treated with 500 μg/mL RNAse-A (Bioke, Leiden, NL) and stained with 0.1 μM of TO-PRO-3-iodide (Invitrogen, Life technologies, Carlsbad, CA, USA) for 15 minutes at 37°C. Cells were acquired on a LSRFortessa cell analyzer (BD Biosciences). Cell cycle distribution was analyzed with the FlowJo 7.6 software (Tree Star, Ashland, OR, USA). The percentage of cells in S phase was determined by BrdU uptake.

2.11 | Western blotting

TECs were lysed in RIPA buffer (50 mM Tris-HCl pH 7.5, 150 mM NaCl, 2 mM EDTA, 1% deoxycholic acid, 1% NP-40, 4 mM sodium orthovanadate, 10 mM sodium fluoride), supplemented with protease and phosphatase inhibitors. Lysates were loaded onto a 4%-12% pre-casted gel and blotted onto a PVDF membrane. The antibodies used were β-actin (Sigma-Aldrich) and cleaved caspase-3 (Cell signaling, Danvers, MA, USA).

2.12 | mRNA extraction and analysis

Total RNA was extracted using TRIzol-reagent (Sigma-Aldrich). cDNA was synthesized using M-MLV reverse transcriptase and oligo-dT primers (Table S1). Transcript analysis was performed by real-time quantitative PCR on a Roche Light Cycler 480 using SYBR green master mix (Bioline, London, UK). Relative expression was analyzed using LinRegPCR.[43] Gene expression was normalized to murine peptidylprolyl isomerase A (*Ppia*) as a housekeeping gene.

2.13 | In vivo study

Animal experiments were performed according to national Dutch and EU ethical guidelines and approved by the local animal experimentation committee under license AVD1180020186906. All the experiments were performed in male C57BL/6N mice at 11 weeks old. Mice were kept in a temperature- and humidity-controlled environment under a 12-hour light/dark cycle with free access to food and water. Twenty-four mice were randomly assigned to three groups and intraperitoneally (IP) injected with saline, NMN or NMNH at 250 mg/kg. Blood was collected from the lateral saphenous vein at 1, 4, and 20 hours after the first IP injection. After 20 hours, another bolus injection was administered and 4 hours after this last injection, mice were sacrificed under isoflurane, and blood and tissues collected and snap frozen in liquid nitrogen until NAD^+ determination and mass spectrometry measurements.

3 | RESULTS

3.1 | Enzymatic synthesis and purification of NMNH

Since NMNH is not commercially available, we developed a preparation method of the compound. To do so, we took advantage of the high activity of the NAD^+ pyrophosphatase from *Escherichia coli* (EcNADD) to cleave NADH into NMNH and AMP[44] (Figure 1A). Indeed, with 2.5 mg of the recombinant enzyme we were able to fully convert 175 mg of NADH into NMNH and AMP in 45 minutes at 37°C (Figure S1A). The two molecules were then successfully separated using C_{18} chromatography (Figure S1B), desalted and freeze dried until an amorphous yellow powder was obtained. The final yield of the process was approximately 70%.

The chemical structure and mass of NMNH were confirmed by UV spectrophotometry, nuclear magnetic resonance (NMR) and mass spectrometry. NMNH was shown to be a fluorescent molecule, in contrast to NMN, with a molar extinction coefficient of 5160 M^{-1} cm^{-1} at 340 nm (Figure 1B), a value that is very similar to that found for the reduced form of nicotinamide riboside (NRH).[45] Structural analysis of NMNH was performed by ^1H and ^{31}P NMR (400 MHz, D_2O; Figure 1C), matching expectations and showing the two characteristic H_4 hydrogens of NMNH

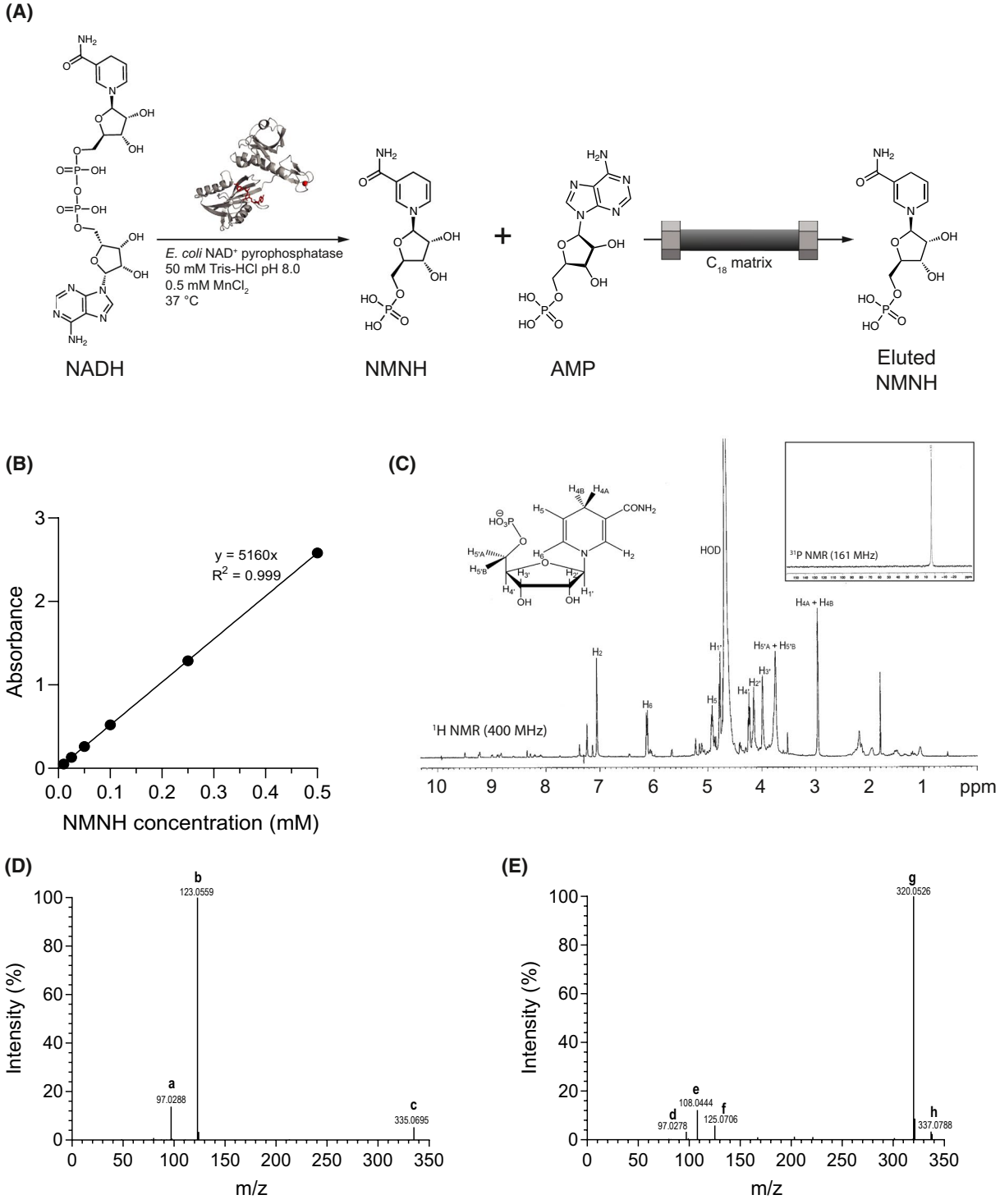

FIGURE 1 NMNH synthesis and characterization. A, Synthesis and purification of NMNH from NADH. B, Linear curve of NMNH concentration vs absorbance at 340 nm. C, ^{1}H and ^{31}P NMR data for NMNH. ^{1}H NMR (400 MHz, D_2O): δ 2.96 (br s, 2H, $H_{4A} + H_{4B}$), 3.75 (br s, 2H, $H_{5A'} + H_{5B'}$), 3.99 (bs s, 1H, $H_{3'}$), 4.13-4.16 (m, 1H, $H_{2'}$), 4.22-4.26 (m, 1H, $H_{4'}$), 4.77-4.79 (m, 1H, $H_{1'}$), 4.86-4.94 (m, 1H, H_5), 6.13 (d, 1H, $J = 8.0$ Hz, H_6), and 7.06 (s, 1H, H_2). Inset: ^{31}P NMR data (161 MHz, D_2O): δ 3.83 (D and E) MS/MS analysis of pure NMN (D) and NMNH (E)

at 3 ppm. NMNH exact mass and fragmentation pattern were analyzed by mass spectrometry in positive ionization mode, using NMN as a reference. As expected, fragmentation patterns were different for each molecule (Figure 1D,E and Table S2), with a major peak corresponding to the nicotinamide component of NMN or the dihydronicotinamide component of NMNH at m/z 123.0559 and m/z 125.0706, respectively. Together, these results confirmed the identity of the purified compound as reduced nicotinamide mononucleotide (NMNH).

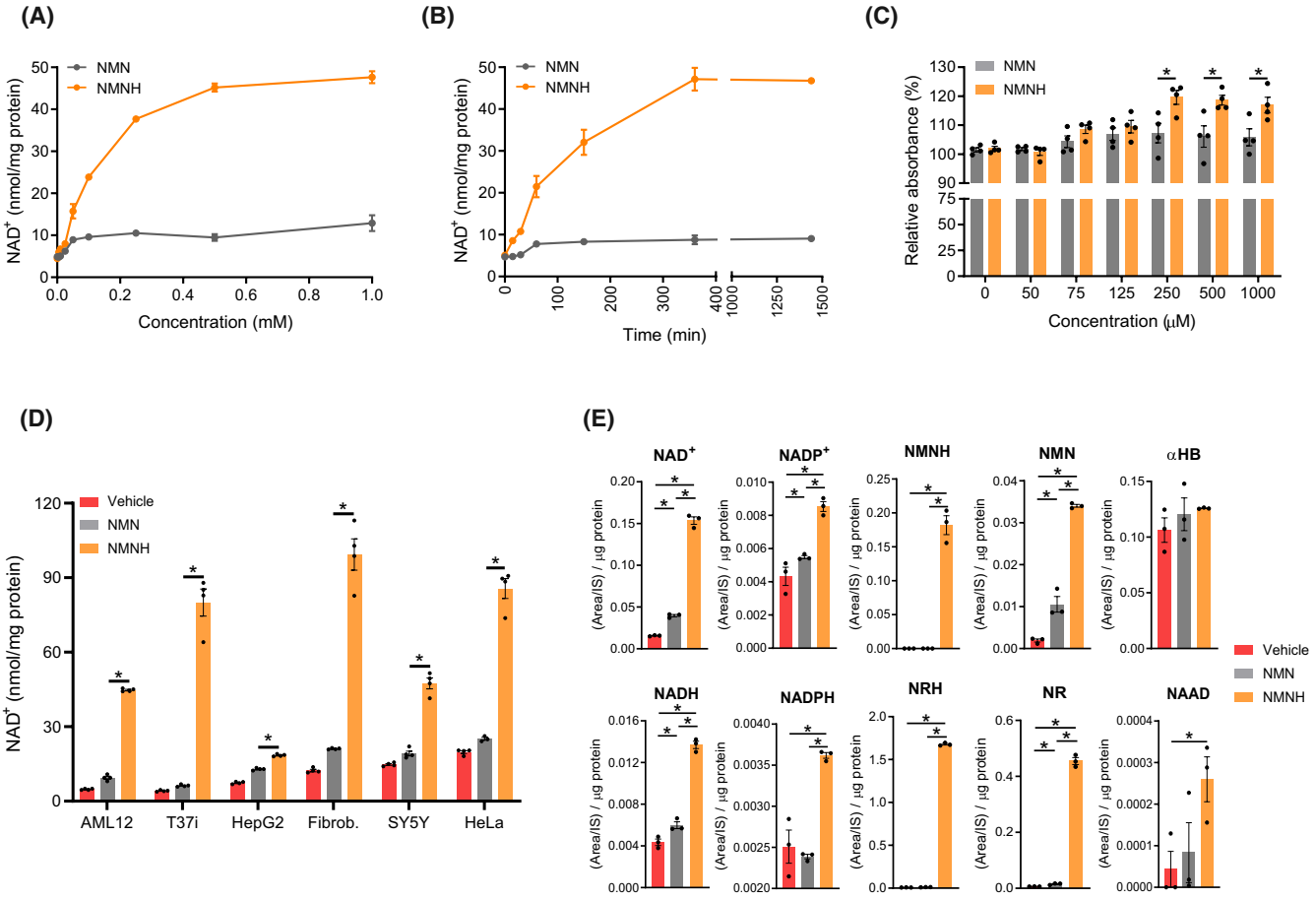

FIGURE 2 NAD$^+$-boosting potential of NMNH. A, AML12 cells were supplemented with increasing concentrations of NMN(H) during 24 hours and collected in 2 M $HClO_4$ for NAD$^+$ measures. B, AML12 cells were supplemented with 500 μM NMN(H) and harvested in 2 M $HCLO_4$ at the indicated time points, followed by NAD$^+$ measurements. C, AML12 cells were supplemented with increasing concentrations of NMN(H) for 24 hours prior to addition of the MTS reagent. Cell survival in the absence of compound (0 μM) was considered as 100% survival (D) AML12, T37i, HepG2, skin fibroblasts, SY5Y, and HeLa cells were supplemented with vehicle (PBS) or 500 μM NMN(H) for 24 hours before acidic extracts were obtained to measure NAD$^+$ levels. E, AML12 cells were treated for 24 hours with vehicle (PBS) or 500 μM NMN(H), and then, quenched in methanol prior to extraction for metabolomics analyses by mass spectrometry. Values are expressed as mean ± SEM of n = 3-4 independent experiments. * indicates a statistical difference of $P < .05$

3.2 | NMNH acts as a potent NAD$^+$ enhancer in vitro

Once we had established a reliable synthesis and purification method and correctly identified the compound obtained as NMNH, our next aim was to test if this reduced precursor was able to act as an NAD$^+$ enhancer in cells. To do so, we supplemented AML12 mouse hepatocytes with different concentrations of either NMN or NMNH. At every concentration tested, NMNH caused a much more significant increase in cellular NAD$^+$ levels than NMN (Figure 2A). In fact, NMNH was able to significantly increase NAD$^+$ at a 10 times lower concentration (5 μM) than that needed for NMN, and reached a plateau at supplementation concentrations of 500 μM. At this concentration, NMNH achieved an almost 10-fold increase in the NAD$^+$ concentration, while NMN was only able to double NAD$^+$ content in these cells, even at 1 mM concentration. NMNH also proved to be a faster precursor, resulting in a significant increase in NAD$^+$ levels within 15 minutes (Figure 2B). Interestingly, upon NMNH supplementation, NAD$^+$ steadily increased for up to 6 hours and remained stable for 24 hours, while NMN reached its plateau after only 1 hour, most likely because the NMN recycling pathways to NAD$^+$ had already become saturated.

We next addressed if such elevation in the NAD$^+$ content could affect the redox balance of the cell, which is crucial for cell survival. For this purpose we used the tetrazolium reagent MTS, which is converted by cellular NAD(P)H-oxidoreductases into formazan colored products.[46] Interestingly, NMNH at concentrations of 250 μM and higher was able to increase absorption at 490 nm, while NMN failed to do so (Figure 2C). These results suggest increased cellular metabolic activity, most likely due to an increase in NAD(P)H levels upon NMNH supplementation.

To further prove that NMNH can act as a potent NAD^+ booster in vitro, we supplemented different murine (AML12 and T37i) and human (HepG2, skin fibroblasts, SY5Y, and HeLa) cell lines with the optimal dose of 500 μM for 24 hours (Figure 2D). NMNH supplementation increased NAD^+ content in all these cell types and was more potent than NMN at the same concentration. While NMN increased NAD^+ levels 1.3-2.4-fold, NMNH outperformed NMN and was able to increase NAD^+ from 2.5-fold in HepG2 hepatocytes, the least responsive cell line, up to 19-fold in the brown adipocytes cell line T37i (Figure 2D). NMNH was also a remarkably potent NAD^+ booster in AML12 hepatocytes (9.3-fold) and fibroblasts (8-fold).

To analyze the effect of NMNH administration on other NAD^+-related metabolites, we performed targeted semi-quantitative metabolomics in AML12 hepatocytes. After 24 hours, NMNH not only led to an increase in NAD^+ levels, but also an enhancement in NADH, although the increase in NADH was less pronounced (~2.8-fold) than that of NAD^+ (~9-fold) (Figure 2E). This result confirms that, as previously described for NRH,[45] NMNH increases NAD^+ content over NADH, leading to a higher NAD^+/NADH balance. In accordance, we could not detect any changes in cellular α-hydroxybutyrate (α-HB) content (Figure 2E), a recently described marker for increased reductive stress.[47]

NMNH supplementation was also accompanied by an increase in $NADP^+$ and NADPH levels, most likely due to the activity of NAD^+ kinase over elevated NAD^+.[48]

Strikingly, NMNH itself could only be detected when it was administered to cells, suggesting that under physiological conditions, this molecule is absent or not detectable with our experimental setup. This was also the case for NRH, which increased only upon NMNH supplementation, suggesting a common metabolism for these two molecules.

Finally, we found an increase in intracellular nicotinic acid adenine dinucleotide (NAAD) (Figure 2E), which is considered as a marker for increased NAD^+ metabolism,[23] as well as increased levels of NMN and NR (Figure 2E), which have been hypothesized to accumulate upon increased NAD^+ synthesis fluxes.[23,49]

3.3 | Identification of enzymes involved in NAD^+ synthesis from NMNH

We next set out to elucidate the enzymatic steps required for the conversion of NMNH to NAD^+. To do so, we measured the ability of NMNH supplementation to increase cellular NAD^+ levels when co-incubated with inhibitors of enzymes or transporters involved in NMN and NR metabolism (Figure 3A). To ensure that each of the inhibitor targets was expressed in the

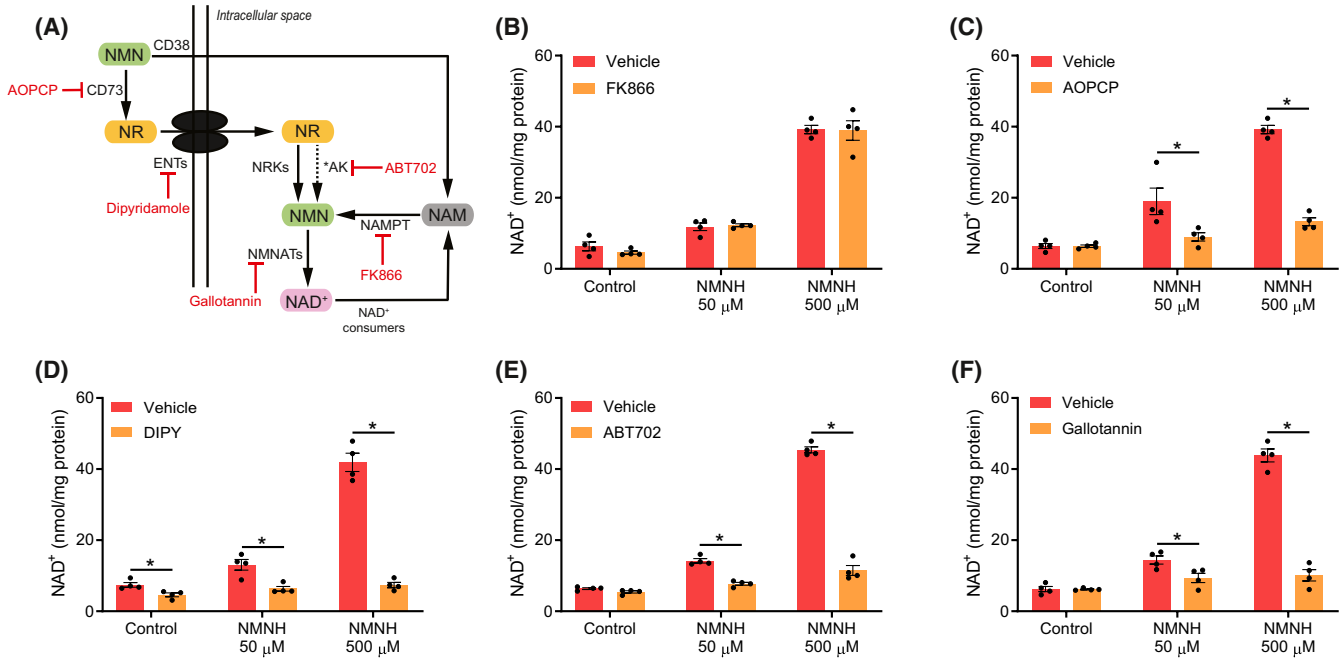

FIGURE 3 Identification of NMNH metabolic pathway to NAD^+. A, NMN and NR recycling pathway to NAD^+ and inhibitors of specific enzymatic steps. *Adenosine kinase (AK) phosphorylation is specific for the conversion of NRH to NMNH. B-F, AML12 cells were treated with inhibitors of NAMPT (FK866; 2 μM), CD73 (AOPCP; 500 μM), ENTs (DIPY; 20 μM), adenosine kinase (ABT702; 10 μM), or NMNATs (Gallotannin; 100 μM) for 1 hour prior to vehicle (PBS) or NMNH supplementation (500 μM) in FBS-free medium. After 24 hours, acidic extracts were obtained to measure NAD^+ levels. Values are expressed as mean ± SEM of n = 4 independent experiments. * indicates a statistical difference of $P < .05$

AML12 cells, we performed qPCR. Indeed, each of the individual targets was expressed in these cells (Figure S2). Next, we investigated the possibility that NMNH could be extracellularly degraded to nicotinamide (NAM), which would then be recycled by the nicotinamide phosphoribosyltransferase (NAMPT) to produce NMN. However, when FK866, an inhibitor of NAMPT, was administered along with NMNH, no differences in NMNH-driven NAD^+ boosting were detected at any of the two concentrations tested (Figure 3B), confirming that NMNH, in contrast to NMN,[8] does not require conversion to NAM to effectively boost NAD^+ in cells.

NMN incorporation into cells can occur through dephosphorylation to NR prior to its uptake by the equilibrative nucleoside transporters (ENTs), and the 5′-nucleotidase CD73 has been identified as the phosphatase involved.[8,30] Our metabolomics analysis already showed that NMNH supplementation also increased NRH content (Figure 2E), pointing toward a convergent metabolic pathway between the two molecules. To confirm that NMNH needs a dephosphorylation step to NRH before incorporation into the cellular NAD^+ pool, we used the specific CD73 inhibitor adenosine-5′-[(α,β)-methylene]diphosphate (AOPCP). Indeed, AOPCP strongly attenuated the NAD^+-boosting effect of NMNH (Figure 3C). Moreover, metabolomics analysis demonstrated that AOPCP supplementation prevents NRH and NMNH accumulation in cells (Figure S3).

We next focused on transport into the cell. NRH metabolization is fully dependent on active transport through equilibrative nucleoside transporters (ENTs).[49] Since NMNH requires a dephosphorylation step to NRH, it seemed likely that ENTs were responsible for this step. To block transport through ENTs we used the specific inhibitor dipyridamole (DIPY) which, even at the highest NMNH concentration, abolished the NAD^+-boosting capacity of NMNH (Figure 3D), and strongly reduced accumulation of NRH and NMNH in cells (Figure S3), demonstrating that transport through the ENTs is essential for NMNH to be incorporated into the cell, and suggesting that NMNH is not incorporated into cells by a different transporter.

In previous work, we showed that NRH was intracellularly metabolized in an NRK and NAMPT-independent pathway.[49] Instead, NRH is phosphorylated back to NMNH by the adenosine kinase (AK), and then, condensed to NADH by the nicotinamide mononucleotide adenylyl transferases (NMNATs).[49] NMNH showed the exact same pattern. Inhibiting AK activity with ABT702 largely reduced NMNH-driven NAD^+ boosting (Figure 3E), an effect also observed when NMNATs were inhibited with gallotannin (Figure 3F). Accordingly, ABT702 supplementation in combination with NMNH led to intracellular NRH accumulation and reduced NMNH production, while gallotannin administration blocked NRH but not NMNH accumulation (Figure S3), demonstrating that the sequential activity of AK and NMNATs is an essential prerequisite for NMNH metabolism to NAD^+.

Together, these results point toward the existence of a convergent pathway between NMNH and NRH, the latter one acting as an intermediate. This pathway shares most of the enzymatic steps that convert oxidized precursors into NAD^+, but is independent of NRKs and NAMPT. This reduced precursor pathway involves CD73-mediated dephosphorylation of NMNH to NRH, which is then taken up by the ENTs and intracellularly phosphorylated back to NMNH by AK, and NMNH is finally converted to NADH by the NMNATs (Figure 3A).

3.4 | NMNH protects tubular epithelial cells against hypoxia/reoxygenation injury by enhancing repair

Within the kidney, the proximal tubular epithelial cells (TECs) are the most vulnerable to ischemic damage, as it directly impacts energy metabolism and poses great pressure on NAD^+ metabolism in TECs. Imbalanced usage of metabolic pathways and the consequent decreased capacity of injured TECs to undergo reparative processes, predispose to kidney disease.[35] Therefore, maintaining NAD^+ homeostasis is crucial for these cells to be able to repair the injured epithelium and to sustain the elevated energy demand for the active transport of substances and reabsorption activity, which together promote healthy kidney function. We tested whether enhancing NAD^+ levels through NMNH administration could aid in the recovery of TECs subjected to hypoxia/reoxygenation injury, an in vitro model of ischemia reperfusion (IR). We first looked at the efficacy of NAD^+ precursors to increase NAD^+ in immortalized proximal TECs exposed to normoxia and hypoxia/reoxygenation. Supplementation with NMNH under normoxic conditions led to a 5-fold increase in the NAD^+ content, whereas at a similar concentration, NMN was only able to double basal levels (Figure 4A). Similarly, both NAD^+ boosters markedly increased NAD^+ levels in hypoxia-challenged TECs (Figure 4A), even to a higher extent than in normoxia, which could be related to metabolic adaptation during hypoxia.[50] Similar to what we observed in cultured hepatocytes, NMNH supplementation in TECs also led to the increase in other NAD^+-related metabolites to a much greater extent than that achieved with NMN (Figure 4B). Additionally, NMNH drives a greater increase in NAD^+ than in NADH, leading to an increase in the NAD^+/NADH ratio in TECs (Figure 4B).

In order to assess the impact of NAD^+ boosting on TEC damage caused by hypoxia/reoxygenation injury, we supplemented TECs with NMN(H) during the reoxygenation

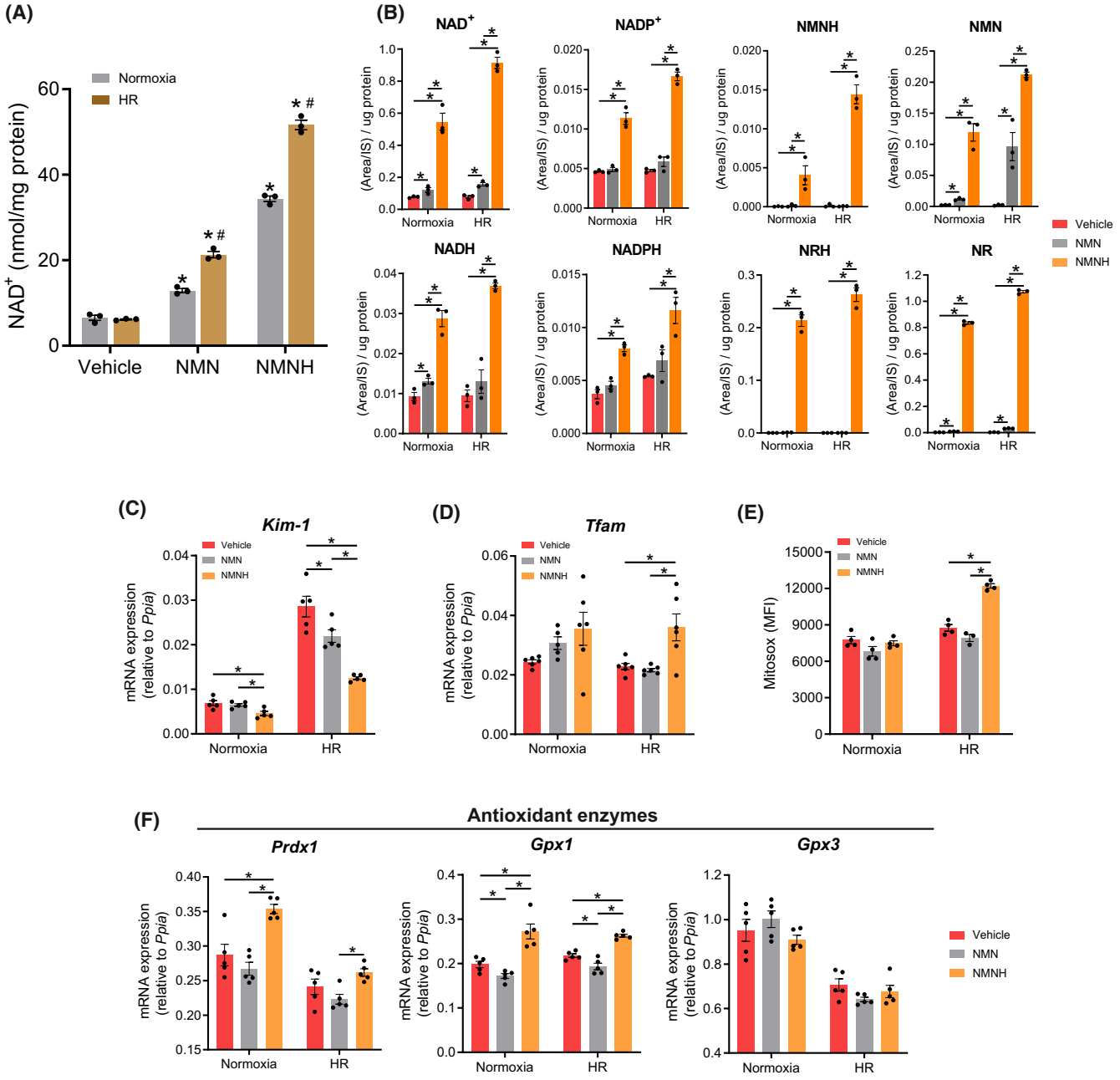

FIGURE 4 Effects of NMN(H) supplementation in an in vitro model of hypoxia/reoxygenation-induced injury. IM-PTECs were subjected to hypoxia or normoxia followed by reoxygenation in the presence of full HK2 medium supplemented with vehicle (PBS) or 500 μM NMN(H). A, NAD^+ levels were measured by spectrophotometry after acidic extraction. B, NAD^+-related metabolites were measured after quenching in methanol prior to extraction for metabolomics analysis by mass spectrometry. C-D, Transcript expression of the tubular damage marker *Kim*-1 (kidney injury molecule 1) and Mitochondrial transcription factor A (*Tfam*). E, Mitochondrial superoxide production measured by FACS using the MitoSox probe. F, Transcript expression of the antioxidant genes: *Gpx* (glutathione peroxidase) 1 and 3, and *Prdx1* (peroxiredoxin 1). Gene expression was measured by RT-PCR. Data are normalized to the reference gene *Ppia* (peptidyl-prolyl cis-trans isomerase A). Values are expressed as mean ± SEM of n = 3-4 independent experiments. * and # indicate a statistical difference of $P < .05$ of treatment vs control or normoxic vs hypoxic conditions, respectively

phase for 24 hours and measured the expression of the widely accepted proximal tubular damage marker KIM-1 (kidney injury molecule-1).[51,52] Reoxygenation in TECs induced a sharp increase in *Kim-1* expression, which was drastically reduced upon NMNH treatment (Figure 4C). To determine if NMNH-driven decrease in tubular damage was dependent on mitochondrial function, we focused our attention on the Mitochondrial Transcription Factor A (*Tfam*). *Tfam* has been recently described to play a crucial role in TECs homeostasis and metabolism via control of mitochondrial activity.[53,54]

Interestingly, NMNH but not NMN supplementation significantly enhanced *Tfam* transcription in TECs during reoxygenation (Figure 4D).

Additionally, mitochondrial damage in TECs can repress oxidative phosphorylation due to deficient electron transfer in the electron transport chain (ETC). In physiological conditions, complex I (NADH dehydrogenase) is the main contributor to mitochondrial superoxide production in the ETC, through both forward or reverse reactions.[55] Using the MitoSox probe, we measured mitochondrial superoxide, generated as a byproduct of the ETC, in normoxic or hypoxia-challenged TECs. Supplementation with vehicle (PBS) or 500 μM NMN(H) was performed during the reoxygenation conditions for 24 hours. Under normoxic conditions, no increase in superoxide production was observed after NMN or NMNH treatment (Figure 4E) in comparison with vehicle-treated cells. However, reoxygenation in the presence of NMNH, but not NMN, promoted a sharp increase in superoxide levels, pointing toward an effect at the ETC level. Taken together, these results suggest that NMNH ameliorates TEC damage, possibly through a functional improvement of mitochondrial activity and restoration of the ETC flux.

To further prove that NMNH-driven superoxide production does not lead to cell damage, we determined the expression of several genes involved in oxidative stress and apoptosis. In this sense, downregulation of the nuclear factor-erythroid 2-related factor 2 (*Nrf2*) or upregulation of the NADPH oxidase 4 (*Nox4*) genes, have been associated with increased ROS production and mitochondrial dysfunction.[56,57] In the same way, an increase in the ratio between Bcl-2-associated X protein (*Bax*) and B-cell lymphoma 2 (*Bcl-2*), or increased cytochrome C (*CytC*) and cleaved caspase-3 expression, are considered markers for cell apoptosis.[58,59] In accordance with previous results, we did not detect changes in the expression of any of these markers upon NMNH supplementation in comparison with vehicle-treated cells (Figure S4). These results suggest that increased production of mitochondrial superoxide by NMNH is the result of ETC recovery and do not cause deleterious effects in TECs.

In highly metabolically active cells like TECs, NAD^+ acts as a hub that coordinates various metabolic pathways,[17] such as the pentose phosphate pathway (PPP), which is involved in cell protection and antioxidant response by modulating the $NADP^+$/NADPH ratio.[60] In fact, an enhanced antioxidant pool is associated with TEC protection against ischemia-reperfusion injury (IRI).[61-64] Since NMNH was able to efficiently increase the $NADP^+$/NADPH ratio in TECs, especially under hypoxic conditions (Figure 4B), we reasoned that it might have impacted their antioxidant capacity. Indeed, the drastic decrease in *Kim-1* expression upon NMNH supplementation was positively correlated with increased transcription of the antioxidant enzymes glutathione peroxidase 1 (*Gpx1*) and peroxiredoxin 1 (*Prdx1*), but not *Gpx3* (Figure 4F).

We then wondered if the activated antioxidant response could be related to increased PPP activity. In TECs, NMNH did not trigger any changes in genes encoding for key enzymes of the oxidative phase of the PPP, such as glucose 6-phosphate 1-dehydrogenase (*G6pdx*) or transketolase (*Tkt*) (Figure S5). However, metabolomics analysis showed accumulation of different products of the non-oxidative phase of the PPP upon reoxygenation (Figure 5A), suggesting increased PPP activity. Interestingly, NMNH supplementation also led to a 3.7-fold accumulation in ribose-5-phosphate. Ribose-5-phosphate is used by phosphoribosyl pyrophosphate (PRPP) synthetase 1 (PRPS1) to generate PRPP, an essential molecule in nucleotide synthesis.[65] In line with this result, we found that NMNH but not NMN supplementation increased the expression of PRPP synthetase 1 (*Prps1*) (Figure S5) and triggered the accumulation of several nucleotides in TECs (Figure 5A), pointing toward increased nucleotide synthesis. Since the metabolic flux through the PPP and the generation of nucleotides is associated with enhanced tubular repair upon renal IRI,[36] we reasoned that the decreased damage and the enhancement of both antioxidant capacity and mitochondrial function observed in the presence of NMNH could have impacted the ability of TECs to repair the damage. By looking at the distribution of the cell cycle phases determined by BrdU incorporation into DNA, we noticed a shift from G1 to S phase in NMNH-treated cells, compared to vehicle and NMN-stimulated cells. Quantification of BrdU-positive (BrdU+) cells (cells in S phase) indicated that NMNH significantly enriched cells at the S phase to prepare for the proliferative stage, and thus, enhanced tubular repair upon hypoxia/reoxygenation injury (Figure 5B-D).

Taken together, our results demonstrate that NMNH supplementation reduces cellular damage in hypoxia/reoxygenation injury and enhances repair by targeting NAD^+ regeneration, mitochondrial activity, and nucleotide metabolism.

3.5 | NMNH efficiently increases NAD^+ levels in vivo

Supplementation with NAD^+ enhancers has emerged as a valid strategy to treat or alleviate features of metabolic and age-related diseases in several preclinical models. To assess the in vivo effects of NMNH in comparison with NMN, we injected C57BL/6N mice with vehicle (PBS) or 250 mg/kg of NMN or NMNH, which was followed by sequential blood sampling (at 1, 4, 20 hours) and, after 24 hours, sacrifice for tissue collection.

NMNH showed a potent NAD^+-boosting effect in blood, efficiently increasing NAD^+ levels after 1 hour and to

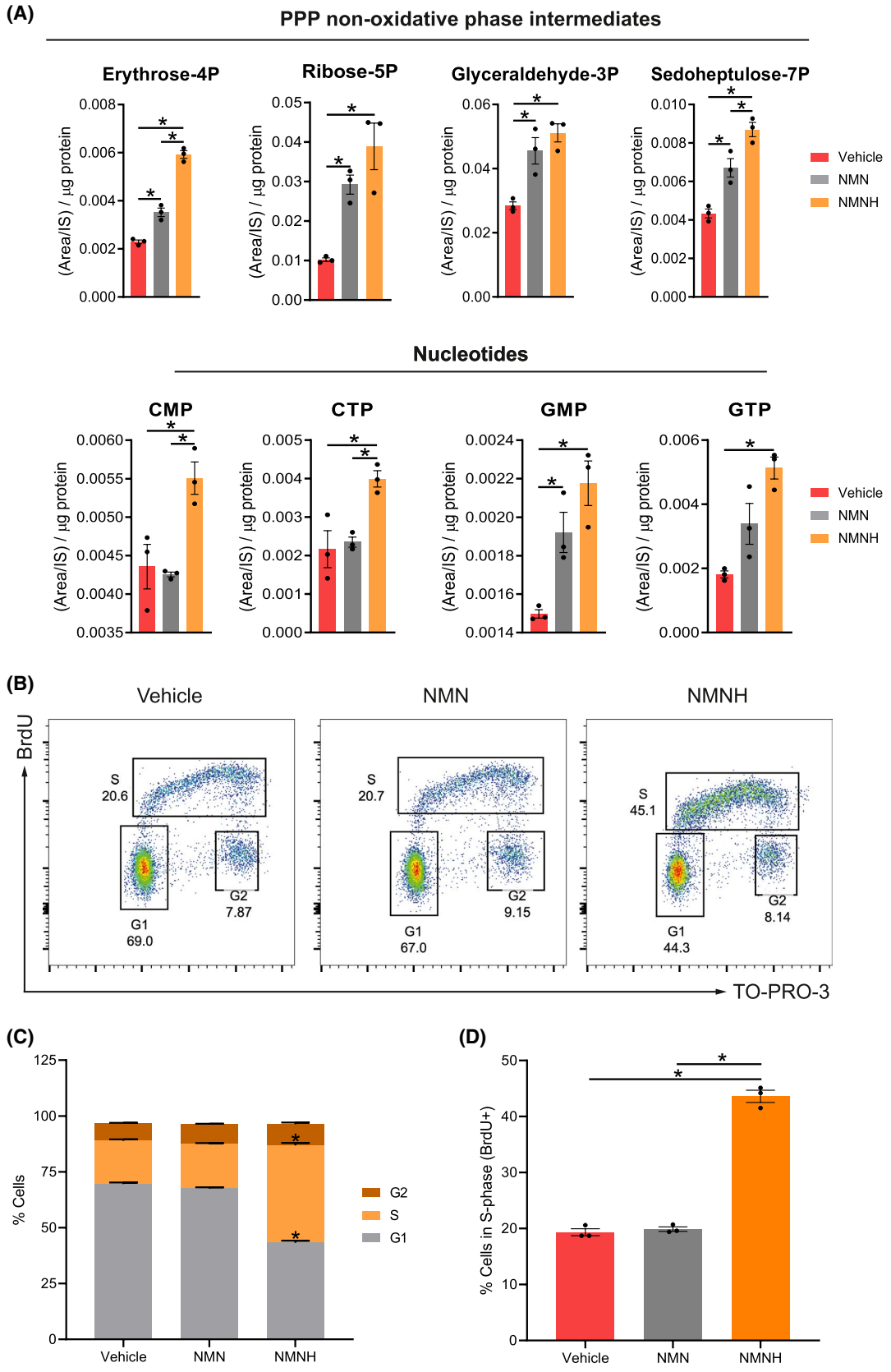

FIGURE 5 Effects of NMN(H) supplementation on the pentose phosphate and nucleotide pathways and on the cell cycle in TECs. IM-PTECs were cultured for 2 days in 1% of oxygen and 5% of CO_2. After 2 days, cells received fresh full HK2 medium supplemented with vehicle (PBS) or the corresponding NAD^+ precursors at 500 µM for 24 hours. A, Cells were quenched in methanol prior to extraction for metabolomics analysis by mass spectrometry. B, Graphical visualization of cell distribution along the three phases of the cell cycle (G1, S, and G2/M) showing a significant enrichment of the S phase upon NMNH supplementation. C, Quantification plot of the cell cycle distribution. D, Percentage of cells in the S phase (BrdU-positive cells). Values are expressed as mean ± SEM of n = 3 independent experiments. * indicates a statistical difference of $P < .05$

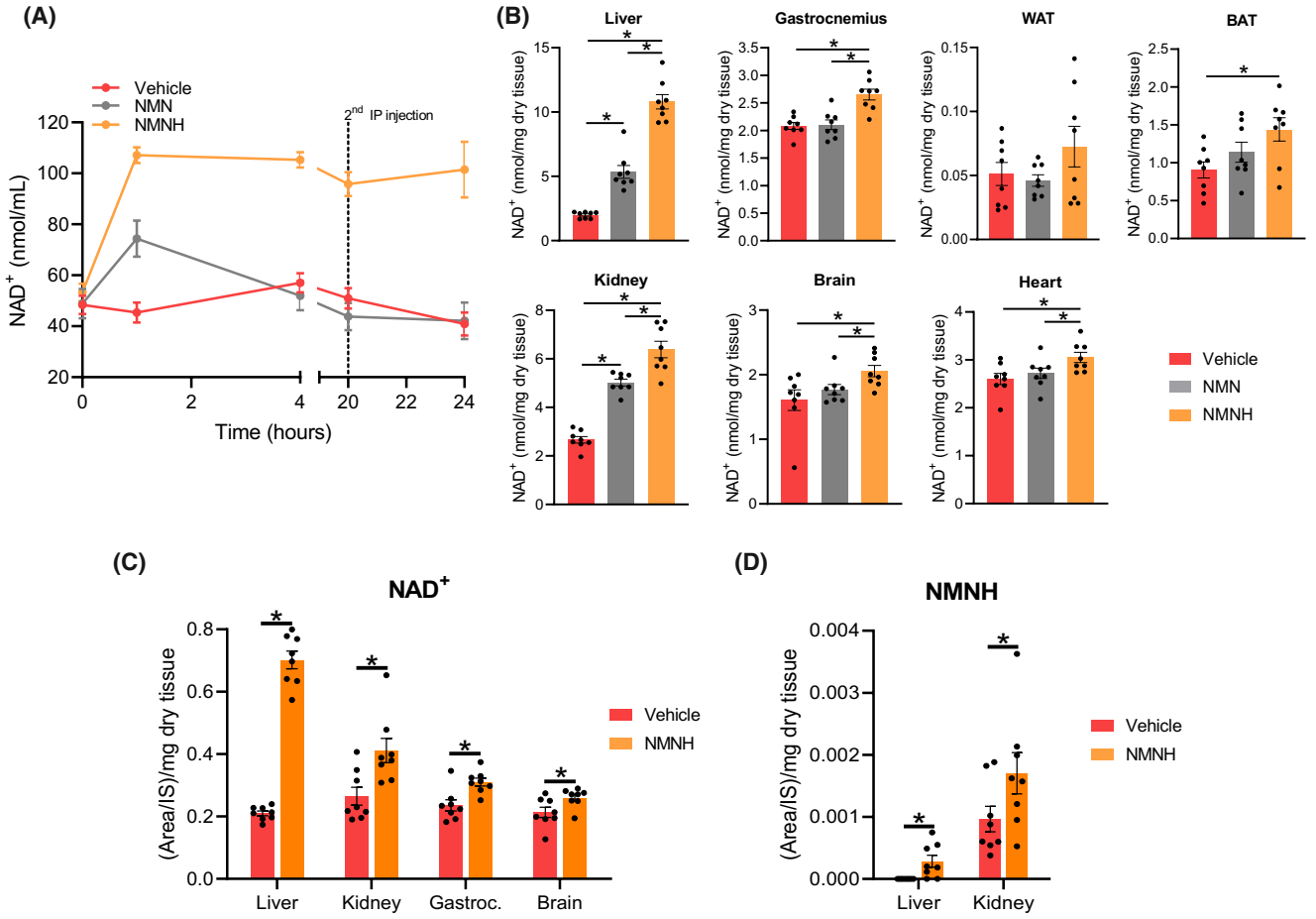

FIGURE 6 In vivo effects of NMN(H) administration. Vehicle (PBS) or 250 mg/kg NMN(H) were administered via intraperitoneal injection. After 20 hours, a second bolus injection was administered at the same concentration and after 4 hours mice were sacrificed for tissue collection. A, Blood NAD^+ profiles obtained at 1, 4, and 20 hours after the first IP injection, and 4 hours after the second IP injection. B, NAD^+ content measured by spectrophotometry after acidic extraction of the freeze-dried tissues. C, NAD^+ abundance in liver, kidney, gastrocnemius muscle, and brain measured by mass spectrometry. D, NMNH abundance in liver and kidney measured by mass spectrometry. Values are expressed as mean ± SEM of n = 8 mice per group. * indicates a statistical difference of $P < .05$

a much higher extent than NMN (Figure 6A). Strikingly, while blood NAD^+ content after NMN supplementation declined to basal levels after just 4 hours, NMNH administration sustained a 2-fold NAD^+ increase for at least 20 hours following the first injection. This was also reflected in the blood samples taken 4 hours after the second IP injection, as an increase in NAD^+ was only detected in NMNH-treated animals (Figure 6A).

We next performed NAD^+ measurements through the enzymatic cycling method on the collected tissues. Our results show that NMNH increased NAD^+ levels in a variety of tissues and to a greater extent than NMN, with the greatest effects in liver (>5-fold increase) and kidney (>2-fold increase) (Figure 6B). NMNH also significantly increased NAD^+ content in other tissues, such as brain, gastrocnemius muscle, brown adipose tissue, and heart, while NMN failed to do so. However, both NAD^+ precursors failed in achieving a significant increase of NAD^+ content in white adipose tissue (Figure 6B). To confirm these results with an independent method, we analyzed liver, kidney, brain, and gastrocnemius samples from untreated and NMNH-treated animals using our mass spectrometry platform. Indeed, with this method we found markedly increased NAD^+ levels in these four tissues (Figure 6C). Finally, we detected NMNH as a naturally occurring precursor, at least in kidney (Figure 6D). We were unable to detect it in the liver, muscle and brain of untreated animals, possibly due to its low abundance or its fast conversion to NAD^+ in these tissues.

Together, our results in mice demonstrate that NMNH is also an efficient NAD^+ booster in vivo that is able to increase NAD^+ levels to a higher extent than NMN in a variety of tissues. Therefore, our study establishes NMNH as the second member of the new family of reduced NAD^+ precursors.

4 | DISCUSSION

NMN and NR are currently the most used and promising NAD^+ modulators, as demonstrated by the many scientific reports showing the benefits of their use in mouse models for cardiometabolic disease,[11,12] fatty liver disease,[15] or neurodegeneration,[16] among many others. The fact that both molecules lack the undesirable side effects of NA (flushing) and NAM (sirtuin inhibition) has increased the interest in the potential use of these compounds as better therapeutic agents. However, supplementation with NR has so far proven to be inefficient in raising NAD^+ levels in human tissue, which could explain why the beneficial effects observed in mouse studies are so far not reproducible in humans.[31] Therefore, new molecules with a higher NAD^+-boosting potential that may overcome these limitations are appealing. This is the case for reduced NR (NRH), which is a very effective NAD^+ booster.[45,49] In the present study, we identify the reduced form of another NAD^+ precursor, namely reduced nicotinamide mononucleotide (NMNH), and show for the first time that it can act as a powerful NAD^+ booster in vitro and in vivo.

To produce NMNH, we leveraged the high activity of the NAD^+ pyrophosphatase from *Escherichia coli* over NADH, and developed an effective purification method that renders salt-free NMNH, whose identity was confirmed by NMR and MS/MS. The molecule proved to be highly efficient and fast in increasing cellular NAD^+, largely surpassing the effect of NMN in every cell line tested. In fact, while NMN was only able to double cellular NAD^+ at its maximum concentration (1 mM), NMNH led to a 3-fold NAD^+ increase even at 50 μM. The response to NMNH was also faster, as 15 minutes were enough for NMNH to almost double basal NAD^+, with maximal effects after 6 hours, which remained stable even 24 hours after supplementation.

This large increase in the NAD^+ pool, which was in the range of 2.5 to 19-fold depending on the cell line, was accompanied by an increase in NADH, although to a much lower extent (~3-fold), suggesting a tight regulation of the NAD^+/NADH ratio in favor of the oxidized form.

The increased NAD^+ metabolic flux is also confirmed by the analysis of downstream NAD^+ metabolites, such as NADP(H) and NAAD, which is considered a marker of increased NAD^+ metabolism.[23] In accordance with these results, and similar to those obtained with NRH,[49] we detected a sharp increase in NMN and NR content upon NMNH supplementation, much higher than that obtained with NMN. This increase in oxidized precursors does not come from oxidation of the reduced ones, as demonstrated previously,[49] but from an increased NAD^+ flux, since blocking NRH conversion to NMNH (and therefore NADH) with an adenosine kinase inhibitor, was enough to prevent NMN and NR accumulation.

In vivo, NMNH also proved more effective than NMN in raising NAD^+ levels in a variety of tissues when administered at the same concentration, confirming the results observed in cell lines.

Our findings solidify the notion that three distinct but partially overlapping NAD^+ recycling pathways exist. In one of these pathways, nicotinic acid (NA) is condensed to NAD^+ via adenylyl transferases (NMNATs) and NAD^+ synthase. In the other two pathways, oxidized precursors (NMN and NR) are converted to NAD^+ through an NR kinases (NRKs) and NAM phosphoribosyltransferase (NAMPT)-dependent route. However, reduced precursors (NMNH and NRH) act independently of these enzymatic activities, and require adenosine kinase (AK) to efficiently increase the cellular NAD^+ pool. We hypothesize that this high efficiency of the reduced pathway could be due to the lack of degradation of the reduced precursors to NAM, which could confer an advantage over the oxidized precursors, since NAM is a weak NAD^+ booster.[30] This hypothesis is further supported by the fact that NMNH was able to sustain NAD^+ levels in blood for much longer than NMN, suggesting reduced degradation to NAM. Another possibility would be an improved cellular uptake of NRH through the ENTs, or a higher efficiency of adenosine kinase or NMN adenylyl transferases for the reduced molecules. These possibilities will need to be addressed in follow-up studies.

In light of the existence of a very efficient pathway for NAD^+ recycling, which leads to unprecedented elevations in the intracellular NAD^+ pool, one question that arises is whether this NAD^+ elevation can lead to deleterious changes in the cellular redox state. In the available studies with NRH, and in the present study with NMNH, this was not the case, as supplementation with NRH or NMNH did not trigger cell apoptosis and instead protected them against genotoxic agents or hypoxia/reoxygenation injury.[45] In accordance, our viability and metabolomics study indicated that NMNH increases metabolic activity by promoting NAD(P)H biosynthesis, without elevating reductive stress, as demonstrated by unchanged levels in α-hydroxybutyrate upon NMNH supplementation.

The data presented in this study also corroborate the evidence that NAD^+ boosters protect against different models of acute kidney injury, and place NMNH as a great alternative intervention to other NAD^+ precursors to reduce tubular damage and accelerate recovery. To demonstrate this point, and with kidney being one of the most responsive tissues to NMNH in vivo, we adopted the in vitro model of hypoxia/reoxygenation injury as a model for damage and repair in TECs, which is the cell type that suffers the most from NAD^+ depletion and mitochondrial dysfunction during ischemic acute kidney injury (AKI).

During reoxygenation, mitochondrial dysfunction and oxidative damage occur in TECs, supposedly as a direct

consequence of ATP depletion due to hypoxia.[66] A marker for aberrant mitochondrial metabolism and disturbed epithelial function is *Tfam*, whose expression is regulated by NAD^+ levels.[67] By efficiently increasing NAD^+ levels, NMNH was also able to promote *Tfam* upregulation and enhance mitochondrial activity, as demonstrated by increased mitochondrial superoxide production. Superoxide can be produced by both forward and reversed electron flux in complex I of the ETC, which in the latter case could exacerbate oxidative damage and cell death. However, our gene expression analysis points toward NMNH-driven protection against hypoxia/reoxygenation injury, as it enhances the expression of the genes encoding for the antioxidant enzymes PRDX1, and GPX1, crucially involved in resistance to renal ischemic damage.[64]

Despite the fact that we did not see upregulation of the genes involved in the pentose phosphate pathway (PPP), our metabolomics results suggest that NMNH supplementation in TECs may enhance antioxidant defense as a result of increased flux through this pathway, yielding necessary intermediates for TEC recovery, such as NADP(H) and nucleotides. In fact, many studies support the role of the PPP in the regeneration of renal tissue after AKI.[36,68-70] We further confirmed this event by showing an enrichment of TECs in the S phase of the cell cycle upon NMNH treatment, which is a sign of cell cycle entry and ongoing repair.[71,72]

Such enhanced repair of TECs in the presence of NMNH is further corroborated by the sharp decrease of the tubular damage marker KIM-1, and is in line with previous findings that NRH also protected against cisplatin-induced acute kidney injury[49] and that other NAD^+-boosting strategies promote tissue regeneration.[73]

In conclusion, owing to an efficient synthesis method for NMNH, we were able to identify this molecule as a new and potent NAD^+ precursor in vitro and in vivo, and confirm the existence of a novel pathway for the recycling of reduced precursors to NAD^+. We have also corroborated the potential therapeutic application of these potent NAD^+ enhancers, which could succeed where NMN and NR have failed, namely boosting NAD^+ in humans. Future research will need to elucidate the safety of long-term administration of reduced precursors, and determine the beneficial effects of their administration in animal models of disease, especially in comparison with the classical boosters.

ACKNOWLEDGMENTS

The authors would like to thank Loes Butter for assistance with hypoxia/reoxygenation assays. AT is financially supported by the NWO-FAPESP joint grant on healthy ageing, executed by ZonMw (no. 457002002). RZP is supported by a postdoctoral grant from the European Union's Horizon 2020 research and innovation program under the Marie Skłodowska-Curie grant agreement number 840110. Work in the Houtkooper group is financially supported by an ERC Starting grant (no. 638290), a VIDI grant from ZonMw (no. 91715305), and a grant from the Velux Stiftung (no. 1063). ASF group is supported by Spanish grants from MINECO-FEDER (BIO2013-45336-R) and from Ayudas a los Grupos y Unidades de Excelencia Científica de la Región de Murcia, Fundación Séneca- Agencia de Ciencia y Tecnología de la Región de Murcia (19893/GERM/15, Programa de Apoyo a la Investigación 2014).

CONFLICT OF INTEREST

JGG and CC are employees of the Nestlé Institute of Health Sciences, which is part of Nestlé Research Ltd. The rest of coauthors declare no conflict of interest.

AUTHOR CONTRIBUTIONS

RZP, AT, JGG, CC, ASF, and RHH conceptualized the project and experiments. RZP, AT, SD, and RLM performed cell-based experiments. RZP, CLL, and ASF performed synthesis and purification experiments and NMR analyses. RZP and AMLS performed the animal experiments. BVS, HLE, and MW developed and performed metabolomics analyses. RZP, AT, and RHH wrote the manuscript, and all authors contributed to its editing.

ORCID

Rubén Zapata-Pérez https://orcid.org/0000-0003-4432-9652
Alessandra Tammaro https://orcid.org/0000-0003-3128-5259
Riekelt H. Houtkooper https://orcid.org/0000-0001-9961-0842

REFERENCES

1. Houtkooper RH, Canto C, Wanders RJ, Auwerx J. The secret life of NAD+: an old metabolite controlling new metabolic signaling pathways. *Endoc Rev*. 2010;31:194-223.
2. Houtkooper RH, Pirinen E, Auwerx J. Sirtuins as regulators of metabolism and healthspan. *Nat Rev Mol Cell Biol*. 2012;13:225-238.
3. Leung AKL. PARPs. *Curr Biol*. 2017;27:R1256-R1258.
4. Wei W, Graeff R, Yue J. Roles and mechanisms of the CD38/cyclic adenosine diphosphate ribose/Ca(2+) signaling pathway. *World J Biol Chem*. 2014;5:58-67.
5. Ansari HR, Raghava GP. Identification of NAD interacting residues in proteins. *BMC Bioinformatics*. 2010;11:160.
6. Mouchiroud L, Houtkooper RH, Auwerx J. NAD(+) metabolism: a therapeutic target for age-related metabolic disease. *Crit Rev Biochem Mol Biol*. 2013;48:397-408.
7. Garavaglia S, Bruzzone S, Cassani C, et al. The high-resolution crystal structure of periplasmic Haemophilus influenzae NAD nucleotidase reveals a novel enzymatic function of human CD73 related to NAD metabolism. *Biochem J*. 2012;441:131-141.
8. Grozio A, Sociali G, Sturla L, et al. CD73 protein as a source of extracellular precursors for sustained NAD+ biosynthesis in FK866-treated tumor cells. *J Biol Chem*. 2013;288:25938-25949.

9. Grozio A, Mills KF, Yoshino J, et al. Slc12a8 is a nicotinamide mononucleotide transporter. *Nat Metab*. 2019;1:47-57.
10. Connell NJ, Houtkooper RH, Schrauwen P. NAD(+) metabolism as a target for metabolic health: have we found the silver bullet? *Diabetologia*. 2019;62:888-899.
11. Canto C, Houtkooper RH, Pirinen E, et al. The NAD(+) precursor nicotinamide riboside enhances oxidative metabolism and protects against high-fat diet-induced obesity. *Cell Metab*. 2012;15:838-847.
12. Yoshino J, Mills KF, Yoon MJ, Imai S. Nicotinamide mononucleotide, a key NAD(+) intermediate, treats the pathophysiology of diet- and age-induced diabetes in mice. *Cell Metab*. 2011;14:528-536.
13. Mouchiroud L, Houtkooper RH, Moullan N, et al. The NAD(+)/Sirtuin pathway modulates longevity through activation of mitochondrial UPR and FOXO signaling. *Cell*. 2013;154:430-441.
14. Zhang H, Ryu D, Wu Y, et al. NAD(+) repletion improves mitochondrial and stem cell function and enhances life span in mice. *Science*. 2016;352:1436-1443.
15. Gariani K, Menzies KJ, Ryu D, et al. Eliciting the mitochondrial unfolded protein response by nicotinamide adenine dinucleotide repletion reverses fatty liver disease in mice. *Hepatology*. 2016;63:1190-1204.
16. Langley B, Sauve A. Sirtuin deacetylases as therapeutic targets in the nervous system. *Neurotherapeutics*. 2013;10:605-620.
17. Ralto KM, Rhee EP, Parikh SM. NAD(+) homeostasis in renal health and disease. *Nat Rev Nephrol*. 2020;16:99-111.
18. Martin DR, Lewington AJ, Hammerman MR, Padanilam BJ. Inhibition of poly(ADP-ribose) polymerase attenuates ischemic renal injury in rats. *Am J Physiol Regul Integr Comp Physiol*. 2000;279:R1834-R1840.
19. Guan Y, Wang SR, Huang XZ, et al. Nicotinamide mononucleotide, an NAD(+) precursor, rescues age-associated susceptibility to AKI in a sirtuin 1-dependent manner. *J Am Soc Nephrol*. 2017;28:2337-2352.
20. Benyo Z, Gille A, Kero J, et al. GPR109A (PUMA-G/HM74A) mediates nicotinic acid-induced flushing. *J Clin Invest*. 2005;115:3634-3640.
21. Khan NA, Auranen M, Paetau I, et al. Effective treatment of mitochondrial myopathy by nicotinamide riboside, a vitamin B3. *EMBO Mol Med*. 2014;6:721-731.
22. Mills KF, Yoshida S, Stein LR, et al. Long-term administration of nicotinamide mononucleotide mitigates age-associated physiological decline in mice. *Cell Metab*. 2016;24:795-806.
23. Trammell SA, Schmidt MS, Weidemann BJ, et al. Nicotinamide riboside is uniquely and orally bioavailable in mice and humans. *Nat Commun*. 2016;7:12948.
24. Martens CR, Denman BA, Mazzo MR, et al. Chronic nicotinamide riboside supplementation is well-tolerated and elevates NAD(+) in healthy middle-aged and older adults. *Nat Commun*. 2018;9:1286.
25. Elhassan YS, Kluckova K, Fletcher RS, et al. Nicotinamide riboside augments the aged human skeletal muscle NAD(+) metabolome and induces transcriptomic and anti-inflammatory signatures. *Cell Rep*. 2019;28:1717-1728.e1716.
26. Airhart SE, Shireman LM, Risler LJ, et al. An open-label, non-randomized study of the pharmacokinetics of the nutritional supplement nicotinamide riboside (NR) and its effects on blood NAD+ levels in healthy volunteers. *PLoS ONE*. 2017;12:e0186459.
27. Conze D, Brenner C, Kruger CL. Safety and metabolism of long-term administration of NIAGEN (Nicotinamide Riboside Chloride) in a randomized, double-blind, placebo-controlled clinical trial of healthy overweight adults. *Sci Rep*. 2019;9:9772.
28. Dollerup OL, Christensen B, Svart M, et al. A randomized placebo-controlled clinical trial of nicotinamide riboside in obese men: safety, insulin-sensitivity, and lipid-mobilizing effects. *Am J Clin Nutr*. 2018;108:343-353.
29. Ryu D, Zhang H, Ropelle ER, et al. NAD+ repletion improves muscle function in muscular dystrophy and counters global PARylation. *Sci Transl Med*. 2016;8:361ra139.
30. Ratajczak J, Joffraud M, Trammell SA, et al. NRK1 controls nicotinamide mononucleotide and nicotinamide riboside metabolism in mammalian cells. *Nat Commun*. 2016;7:13103.
31. Remie CME, Roumans KHM, Moonen MPB, et al. Nicotinamide riboside supplementation alters body composition and skeletal muscle acetylcarnitine concentrations in healthy obese humans. *Am J Clin Nutr*. 2020;112(2):413-426.
32. Abdelraheim SR, Spiller DG, McLennan AG. Mammalian NADH diphosphatases of the Nudix family: cloning and characterization of the human peroxisomal NUDT12 protein. *Biochem J*. 2003;374:329-335.
33. Abdelraheim SR, Spiller DG, McLennan AG. Mouse Nudt13 is a mitochondrial nudix hydrolase with NAD(P)H pyrophosphohydrolase activity. *Protein J*. 2017;36:425-432.
34. Berger F, Lau C, Dahlmann M, Ziegler M. Subcellular compartmentation and differential catalytic properties of the three human nicotinamide mononucleotide adenylyltransferase isoforms. *J Biol Chem*. 2005;280:36334-36341.
35. Tammaro A, Kers J, Scantlebery AML, Florquin S. Metabolic flexibility and innate immunity in renal ischemia reperfusion injury: the fine balance between adaptive repair and tissue degeneration. *Front Immunol*. 2020; 11:1346.
36. Scantlebery AM, Tammaro A, Mills JD, et al. The dysregulation of metabolic pathways and induction of the pentose phosphate pathway in renal ischaemia reperfusion injury. *J Pathol*. 2020. https://doi.org/10.1002/path.5605. [Epub ahead of print].
37. Nakae J, Cao Y, Oki M, et al. Forkhead transcription factor FoxO1 in adipose tissue regulates energy storage and expenditure. *Diabetes*. 2008;57:563-576.
38. Zennaro MC, Le Menuet D, Viengchareun S, Walker F, Ricquier D, Lombes M. Hibernoma development in transgenic mice identifies brown adipose tissue as a novel target of aldosterone action. *J Clin Invest*. 1998;101:1254-1260.
39. Stokman G, Stroo I, Claessen N, et al. Stem cell factor expression after renal ischemia promotes tubular epithelial survival. *PLoS ONE*. 2010;5:e14386.
40. Pulskens WP, Teske GJ, Butter LM, et al. Toll-like receptor-4 coordinates the innate immune response of the kidney to renal ischemia/reperfusion injury. *PLoS ONE*. 2008;3:e3596.
41. Stokman G, Qin Y, Genieser HG, et al. Epac-Rap signaling reduces cellular stress and ischemia-induced kidney failure. *J Am Soc Nephrol*. 2011;22:859-872.
42. Kato T, Berger SJ, Carter JA, Lowry OH. An enzymatic cycling method for nicotinamide-adenine dinucleotide with malic and alcohol dehydrogenases. *Anal Biochem*. 1973;53:86-97.
43. Ruijter JM, Ramakers C, Hoogaars WM, et al. Amplification efficiency: linking baseline and bias in the analysis of quantitative PCR data. *Nucleic Acids Res*. 2009;37:e45.
44. Frick DN, Bessman MJ. Cloning, purification, and properties of a novel NADH pyrophosphatase. Evidence for a nucleotide pyrophosphatase catalytic domain in MutT-like enzymes. *J Biol Chem*. 1995;270:1529-1534.

45. Yang Y, Mohammed FS, Zhang N, Sauve AA. Dihydronicotinamide riboside is a potent NAD(+) concentration enhancer in vitro and in vivo. *J Biol Chem*. 2019;294:9295-9307.
46. Riss TL, Moravec RA, Niles AL, et al. Cell viability assays. In: Sittampalam GS, Grossman A, Brimacombe K, Arkin M, Auld D, Austin CP, Baell J, Bejcek B, Caaveiro JMM, Chung TDY, Coussens NP, Dahlin JL, Devanaryan V, Foley TL, Glicksman M, Hall MD, Haas JV, Hoare SRJ, Inglese J, Iversen PW, Kahl SD, Kales SC, Kirshner S, Lal-Nag M, Li Z, McGee J, McManus O, Riss T, Saradjian P, Trask OJ, Weidner JR, Wildey MJ, Xia M, Xu X, eds. *Assay Guidance Manual*. Bethesda, MD: Eli Lilly & Company and the National Center for Advancing Translational Sciences; 2004.
47. Goodman RP, Markhard AL, Shah H, et al. Hepatic NADH reductive stress underlies common variation in metabolic traits. *Nature*. 2020;583(7814):122-126.
48. Love NR, Pollak N, Dolle C, et al. NAD kinase controls animal NADP biosynthesis and is modulated via evolutionarily divergent calmodulin-dependent mechanisms. *Proc Natl Acad Sci USA*. 2015;112:1386-1391.
49. Giroud-Gerbetant J, Joffraud M, Giner MP, et al. A reduced form of nicotinamide riboside defines a new path for NAD(+) biosynthesis and acts as an orally bioavailable NAD(+) precursor. *Molec Metab*. 2019;30:192-202.
50. Lan R, Geng H, Singha PK, et al. Mitochondrial Pathology and Glycolytic Shift during Proximal Tubule Atrophy after Ischemic AKI. *J Am Soc Nephrol*. 2016;27:3356-3367.
51. Ichimura T, Bonventre JV, Bailly V, et al. Kidney injury molecule-1 (KIM-1), a putative epithelial cell adhesion molecule containing a novel immunoglobulin domain, is up-regulated in renal cells after injury. *J Biol Chem*. 1998;273:4135-4142.
52. Bonventre JV. Kidney injury molecule-1: a translational journey. *Trans Am Clin Climatol Assoc*. 2014;125:293-299; discussion 299.
53. Huang S, Park J, Qiu C, et al. Jagged1/Notch2 controls kidney fibrosis via Tfam-mediated metabolic reprogramming. *PLoS Biol*. 2018;16:e2005233.
54. Chung KW, Dhillon P, Huang S, et al. Mitochondrial damage and activation of the STING pathway lead to renal inflammation and fibrosis. *Cell Metab*. 2019;30:784-799.e785.
55. Brand MD, Affourtit C, Esteves TC, et al. Mitochondrial superoxide: production, biological effects, and activation of uncoupling proteins. *Free Radic Biol Med*. 2004;37:755-767.
56. Ren HL, Lv CN, Xing Y, et al. Downregulated nuclear factor E2-related Factor 2 (Nrf2) aggravates cognitive impairments via neuroinflammation and synaptic plasticity in the senescence-accelerated mouse Prone 8 (SAMP8) mouse: a model of accelerated senescence. *Med Sci Monit*. 2018;24:1132-1144.
57. Ago T, Kuroda J, Pain J, Fu C, Li H, Sadoshima J. Upregulation of Nox4 by hypertrophic stimuli promotes apoptosis and mitochondrial dysfunction in cardiac myocytes. *Circ Res*. 2010;106:1253-1264.
58. Yang B, Johnson TS, Thomas GL, et al. Expression of apoptosis-related genes and proteins in experimental chronic renal scarring. *J Am Soc Nephrol*. 2001;12:275-288.
59. Elena-Real CA, Diaz-Quintana A, Gonzalez-Arzola K, et al. Cytochrome c speeds up caspase cascade activation by blocking 14-3-3epsilon-dependent Apaf-1 inhibition. *Cell Death Dis*. 2018;9:365.
60. Xiao W, Wang RS, Handy DE, Loscalzo J. NAD(H) and NADP(H) redox couples and cellular energy metabolism. *Antioxidant Redox Signal*. 2018;28:251-272.
61. Paller MS, Patten M. Protective effects of glutathione, glycine, or alanine in an in vitro model of renal anoxia. *J Am Soc Nephrol*. 1992;2:1338-1344.
62. Mandel LJ, Schnellmann RG, Jacobs WR. Intracellular glutathione in the protection from anoxic injury in renal proximal tubules. *J Clin Invest*. 1990;85:316-324.
63. Zhou HL, Zhang R, Anand P, et al. Metabolic reprogramming by the S-nitroso-CoA reductase system protects against kidney injury. *Nature*. 2019;565:96-100.
64. Ishibashi N, Weisbrot-Lefkowitz M, Reuhl K, Inouye M, Mirochnitchenko O. Modulation of chemokine expression during ischemia/reperfusion in transgenic mice overproducing human glutathione peroxidases. *J Immunol*. 1999;163:5666-5677.
65. Hosios AM, Vander Heiden MG. The redox requirements of proliferating mammalian cells. *J Biol Chem*. 2018;293:7490-7498.
66. Devarajan P. Update on mechanisms of ischemic acute kidney injury. *J Am Soc Nephrol*. 2006;17:1503-1520.
67. Gomes AP, Price NL, Ling AJ, et al. Declining NAD(+) induces a pseudohypoxic state disrupting nuclear-mitochondrial communication during aging. *Cell*. 2013;155:1624-1638.
68. Cao L, Zhang D, Chen J, et al. G6PD plays a neuroprotective role in brain ischemia through promoting pentose phosphate pathway. *Free Radic Biol Med*. 2017;112:433-444.
69. Ash SR, Cuppage FE. Shift toward anaerobic glycolysis in the regenerating rat kidney. *Am J Pathol*. 1970;60:385-402.
70. Kim J, Devalaraja-Narashimha K, Padanilam BJ. TIGAR regulates glycolysis in ischemic kidney proximal tubules. *Am J Physiol Renal Physiol*. 2015;308:F298-308.
71. Khamchun S, Thongboonkerd V. Cell cycle shift from G0/G1 to S and G2/M phases is responsible for increased adhesion of calcium oxalate crystals on repairing renal tubular cells at injured site. *Cell Death Discov*. 2018;4:106.
72. Yang L, Besschetnova TY, Brooks CR, Shah JV, Bonventre JV. Epithelial cell cycle arrest in G2/M mediates kidney fibrosis after injury. *Nat Med*. 2010;16:535-543, 531p following 143.
73. Mukherjee S, Chellappa K, Moffitt A, et al. Nicotinamide adenine dinucleotide biosynthesis promotes liver regeneration. *Hepatology*. 2017;65:616-630.

SUPPORTING INFORMATION

Additional Supporting Information may be found online in the Supporting Information section.

How to cite this article: Zapata-Pérez R, Tammaro A, Schomakers BV, et al. Reduced nicotinamide mononucleotide is a new and potent NAD^+ precursor in mammalian cells and mice. *The FASEB Journal*. 2021;35:e21456. https://doi.org/10.1096/fj.202001826R